

Practical limits to thermophotovoltaic efficiency

Zunaid Omair



Electrical Engineering and Computer Sciences
University of California, Berkeley

Technical Report No. UCB/EECS-2022-8

<http://www2.eecs.berkeley.edu/Pubs/TechRpts/2022/EECS-2022-8.html>

May 1, 2022

Copyright © 2022, by the author(s).
All rights reserved.

Permission to make digital or hard copies of all or part of this work for personal or classroom use is granted without fee provided that copies are not made or distributed for profit or commercial advantage and that copies bear this notice and the full citation on the first page. To copy otherwise, to republish, to post on servers or to redistribute to lists, requires prior specific permission.

Acknowledgement

Experimental design, measurement, and data analysis were supported by Department of Energy (DOE) “Light-Material Interactions in Energy Conversion” Energy Frontier Research Center under Grant DE-SC0001293 and DOE “Photonics at Thermodynamic Limit” Energy Frontier Research Center under Grant DE-SC00019140.

Practical limits to thermophotovoltaic efficiency

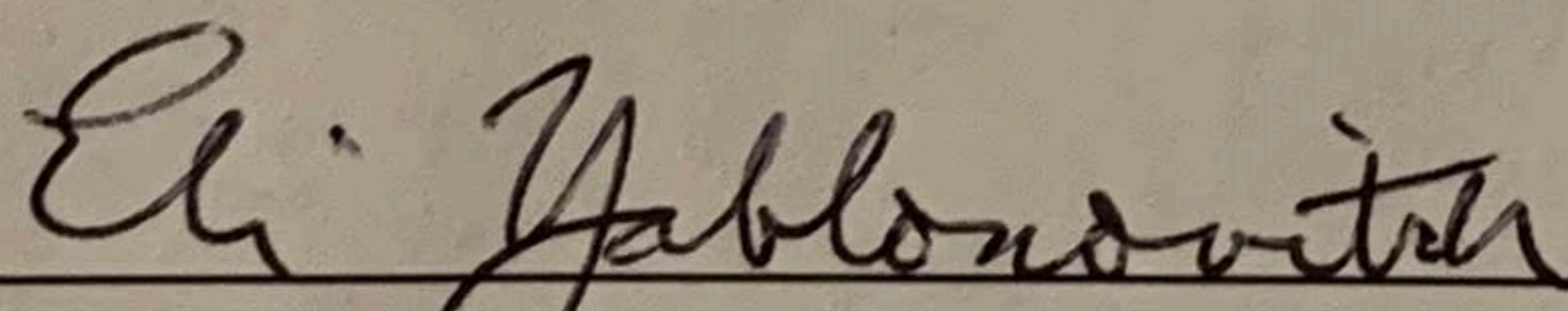
by Zunaid Omair

Project on Ultra-efficient thermophotovoltaics

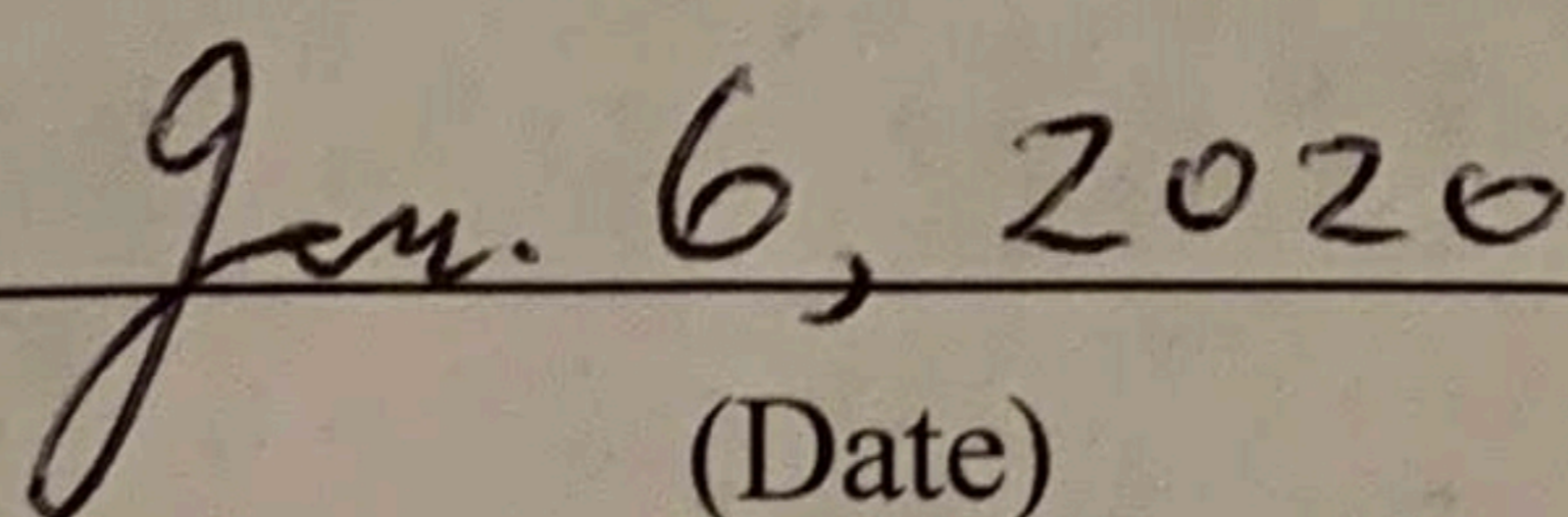
Submitted to the Department of Electrical Engineering and Computer Sciences,
University of California at Berkeley, in partial satisfaction of the requirements for the
degree of **Master of Science, Plan II.**

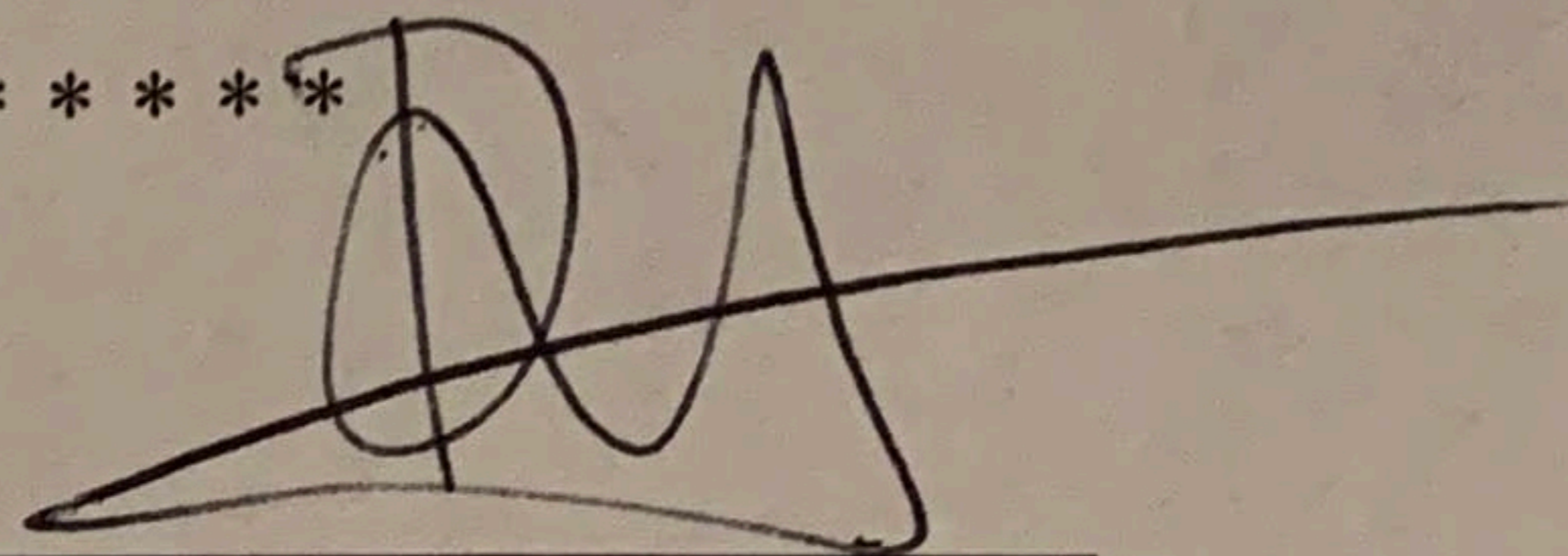
Approval for the Report and Comprehensive Examination:

Committee:

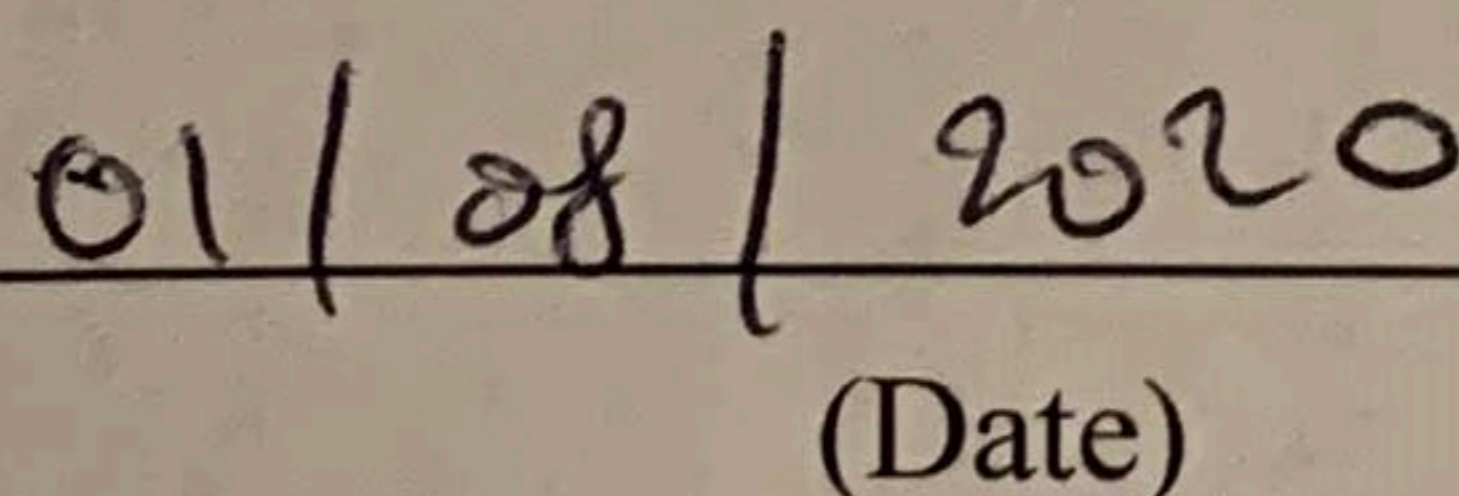


Professor Eli Yablonovitch
Research Advisor


(Date)



Professor Boubacar Kanté
Second Reader


(Date)

ABSTRACT

A highly reflective rear mirror can increase the efficiency of thermophotovoltaics through the regeneration of unused photons. Based on this concept, we recently demonstrated a record 29.1% thermophotovoltaic device efficiency. We have also identified the challenges as we aim towards 50% thermophotovoltaic efficiency, mainly device sub-bandgap reflectivity, material quality, carrier collection as well as test chamber geometry. Here, we present an analysis of each of these factors, and ways to mitigate these challenges.

Practical limits to thermophotovoltaic efficiency

1 Introduction

Thermophotovoltaics utilizes photovoltaic cells to extract electricity from the blackbody radiation of a hot emitter. The radiation from the emitter spans over a broadband spectrum. However, the semiconductor absorbers in the photovoltaic cell are only able to absorb and utilize the photons with energies greater than the band-gap of the semiconductor (Fig. 1). Any photons with energies less than the band-gap of the semiconductor will otherwise be wasted. For an emitter at 1200°C and with a lattice-matched InGaAs photovoltaic cell ($E_g = 0.75\text{eV}$), it is only possible to obtain 8% heat to electricity conversion efficiency.

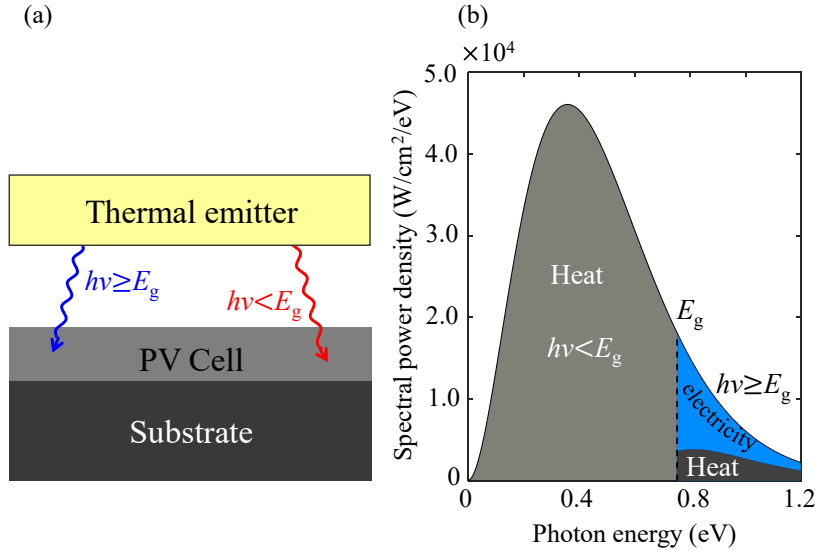


Figure 1. Thermophotovoltaic power conversion. A hot blackbody emitter radiates photons over a broad spectrum. Only the photons with energies above the bandgap are utilized for electricity generation.

To minimize the loss associated with low energy photons, different schemes have been utilized. One approach has been to tailor the emission spectrum of the thermal emitter. The objective is to suppress the emissions of low-energy photons, as shown in Fig. 2(a). People have used nanostructured metamaterials [1] and photonic crystals [2] for this purpose.

A second approach has been to use a highly reflective mirror at the back of the photovoltaic cell. Any photon that is not being absorbed by the photovoltaic cell will be reflected to the emitter, where it can be reabsorbed. The photon can then be re-emitted (Fig. 2b). The process ensures the regeneration of photons, thereby minimizing photon loss. Power conversion efficiency is given as

$$\eta = \frac{P_{\text{electrical}}}{P_{\text{incident}} - P_{\text{reflected}}} \quad (1)$$

where $P_{\text{electrical}}$ is the electrical power generated by the photovoltaic cell, P_{incident} is the power incident on the cell, and $P_{\text{reflectivity}}$ is the reflected power from the cell. As such, higher is the reflectivity (and the reflected power), higher is the thermophotovoltaic efficiency. Previously researchers from Bechtel Bettis Inc. demonstrated a power conversion efficiency of 23% based on this method. The reflectivity of the rear mirror was 90% for that experiment. We recently demonstrated [3] a new thermophotovoltaic efficiency record of 29.1%, with photovoltaic cells that have an average reflectivity of 94.6%.

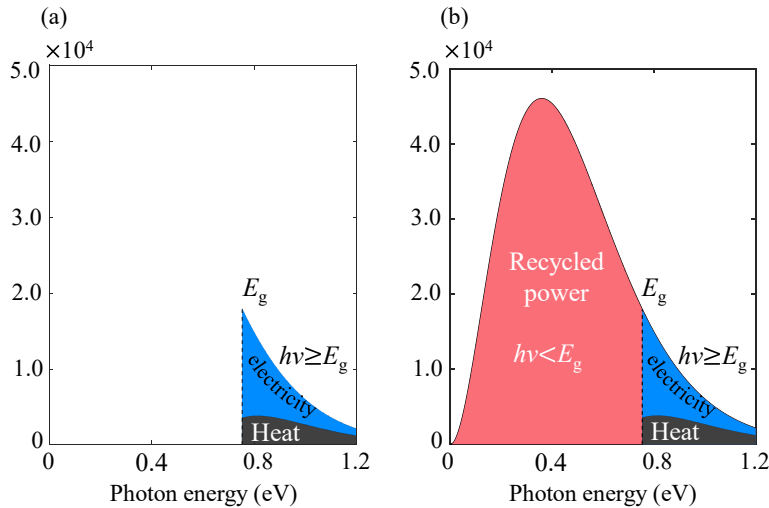


Figure 2. Increasing thermophotovoltaic efficiency. One approach is to reduce the emission of sub-bandgap photons (a). A simpler approach (b) would be to use a rear mirror to regenerate any unused photons, with energies below the band-gap.

A closer look at the physics shows that it is possible to achieve >50% efficiency in this approach. In Fig. 3, the power conversion efficiency is plotted against the mirror reflectivity. We have also shown the optimum bandgap for each mirror reflectivity. For a given emitter temperature, as the mirror reflectivity is increased, the optimal bandgap also increases. Any deviation from 100% reflectivity will introduce a mirror loss in the below-bandgap part of the spectrum. Apart from that, in the high energy part of the spectrum (above E_g), the main sources of loss are the thermalization of high energy carriers, defect-induced Shockley-Read-Hall recombination and voltage loss due to entropy generation. Improvements in mirror reflectivity reduce the loss in the below-bandgap part of the spectrum. As such, with increased reflectivity of the mirror, the losses in the above-bandgap part become more prominent. An increase in semiconductor bandgap, therefore, reduces the relative contribution of loss from the above-bandgap part of the spectrum. This is the reasoning behind an increase in optimal bandgap with an increase in mirror reflectivity.

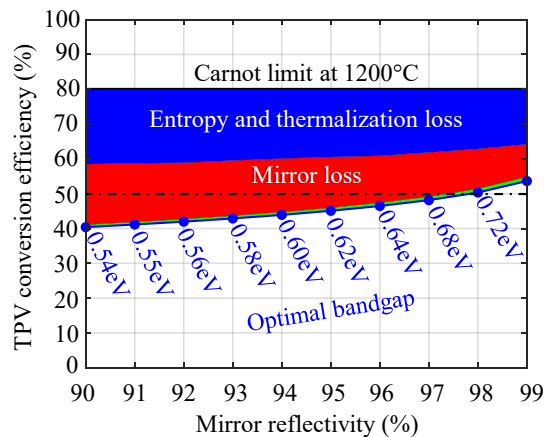


Figure 3. Optimum bandgap for thermophotovoltaics. For an emitter at 1200°C, it is possible to obtain more than 50% power conversion efficiency, with >98% rear mirror reflectivity. For this calculation, we used 98% internal luminescence efficiency, and zero series resistance for the device. The effects of the material loss appear as the thin green sliver on the graph.

For the calculation in Fig. 3, we assumed zero series resistance and unity emissivity of the emitter. We used an internal luminescence efficiency—the probability that photons inside the semiconductor undergo radiative recombination—of 98%. Such internal luminescence efficiency is representative of an inherently Auger-limited InGaAs. We will discuss the effects of series resistance and non-unity emissivity in later sections.

The noteworthy observation from Fig. 3 is that it predicts a ~50% efficiency with a mirror reflectivity of >98%. This corresponds to an optimal bandgap ~0.74eV. For our experiments at 29.1% efficiency, the active layer of the semiconductor was $\text{In}_{0.55}\text{Ga}_{0.45}\text{As}$, which has an optical bandgap of 0.74eV. However, even with a 94%

reflective mirror, we achieved 29.1% efficiency. This brings us to the question of why the efficiency is limited to 29.1%, and what are the practical limits of thermophotovoltaic energy conversion?

In the next sections, we will show the factors limiting the performances of our device to 29.1%. We will also describe ways to circumvent or improve these limitations.

2 Path to 50% thermophotovoltaic efficiency

We have plotted our experimental results (blue dots) against the modeling predictions (blue line) in Fig. 4. The input parameters to the model were the measured reflectivity ($R=94.6\%$), measured series resistance ($R_s=0.43\Omega$) from the dark IV curve and the effective view factor ($F_{\text{view}}=0.31$). The internal luminescence efficiency ($\eta_{\text{int}}=82\%$) was not directly measured. It was obtained from the measured short-circuit current and the reflectivity spectrum of the device. The detailed procedure is described in the supplementary section of [3].

The intrinsic series resistances of the devices were 0.1Ω ($10\text{m}\Omega\text{-mm}^2$, the surface area of the cells were $\sim 10\text{mm}^2$). The devices were wire-bonded for efficiency measurements. The resulting series resistance from the wire bonds were 0.43Ω . This excess series resistance resulted in a loss of fill-factor, and thereby thermophotovoltaic efficiency. Additionally, the view factor—solid angle subtended by the cell as viewed from the emitter—was 0.31 . When these two non-idealities are removed, TPV efficiency increases further, as noted by the red line in Fig. 4.

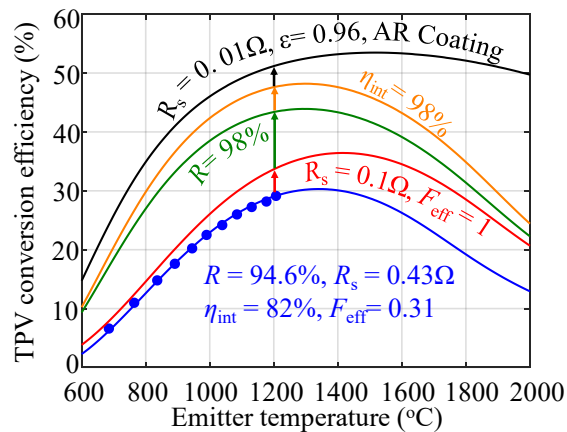


Figure 4. Path to higher thermophotovoltaic efficiency. Improvements in mirror reflectivity, series resistance, material quality in the device, as well as an improved chamber geometry can lead to $>50\%$ efficiency as shown in Fig. 3.

One important point to note about the series resistance is the effect on the high emitter temperature regime. If we compare the slope of the blue and the red curve for emitter temperatures $>1400^\circ\text{C}$, efficiency for the blue line decreases faster. This difference is due to the higher series resistance in our devices. Higher resistance penalizes more strongly at high emitter temperatures. At those temperatures, current crowding starts to degrade the fill-factor severely, due to higher generation rate inside the device.

For our devices, we measured series resistance by taking the slope of the I-V curve measured under dark and then subtracting the slope of the quasi-Fermi level. Mathematically, we can express this as,

$$R_s = \frac{dV}{dI} - \frac{V_T}{I} \quad (2)$$

where V_T is the thermal voltage ($K_b \cdot T/q$). Since we have an ohmic contact due to the use of a highly doped contact layer, the series resistance for the dark measurement can be assumed to be the same as for measurements done under illumination. In the presence of a Schottky contact, this assumption would not hold.

Once, we have taken into consideration the non-idealities in our measurement, we can look towards improving the device parameters.

2.1 Sub-bandgap Reflectivity

Regenerative thermophotovoltaics relies on a highly reflective mirror for sub-bandgap photons. For a simple semiconductor-metal interface, theory predicts a maximum reflectivity of 94-95%. This is quite close to the value we obtained for our device (94.6% on average). This limitation comes from a lower refractive index contrast for the semiconductor-metal structure, compared to an air-metal interface. This can be solved by having a layer of low-index (compared to the refractive index of the semiconductor). The results are shown in Fig. 5 (a). The blue line corresponds to an InGaAs-Gold structure, whereas the red line shows the reflectivity of InGaAs-SiO₂-Gold structure.

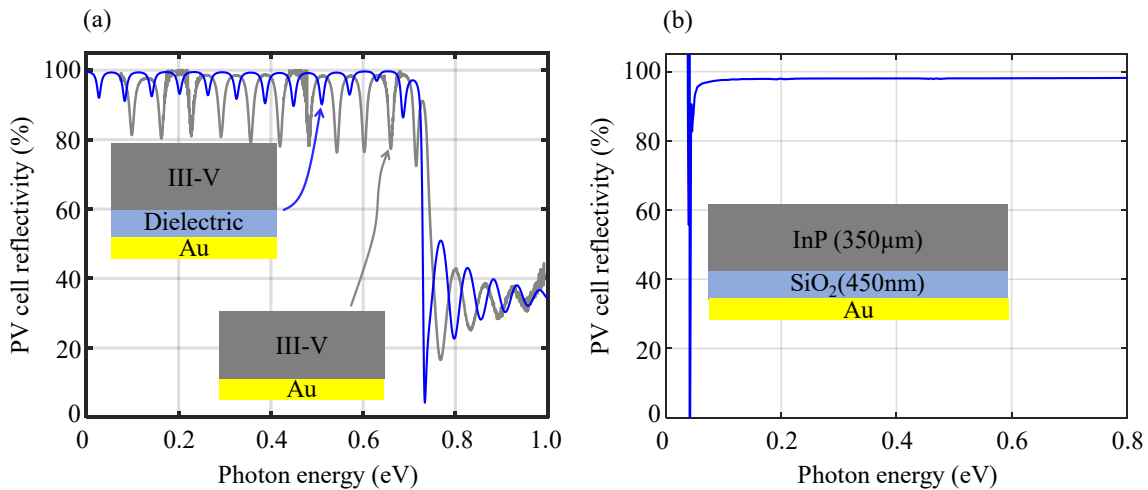


Figure 5. Improving the rear mirror reflectivity. It is possible to improve the mirror reflectivity to 98% through the addition of a dielectric layer between semiconductor and metal, as shown in (a). The dielectric-metal mirror under an InP superstrate resulted in 98% reflectivity experimentally, as shown in (b). The interference fringes are not present in (b) due to the thick superstrate. Also, the phonon absorption in the thick superstrate is also visible in the measured reflectivity spectrum, at ~0.05 eV.

The average reflectivity in the latter case is 98%, for an optimized SiO₂ thickness of 450 nm. Optimization was performed for an emitter temperature of 1200 °C. The dielectric-mirror metal was later grown via PECVD and e-beam deposition, respectively, on an InP superstrate. The reflectivity spectrum is shown in Fig. 5(b).

2.2 Series Resistance

Series resistance can drastically penalize the fill-factors of the device, given the high carrier generation rate in thermophotovoltaic cells. For our experiments, the emitter at 1200 °C created a carrier density equivalent to 128 suns inside the thermophotovoltaic cell. At such concentration, reducing series resistance becomes a critical component of the device design. We had gold cross-bars for the cathode at the top of the cell, and the anode was a plane gold layer. The cross-bar resistance, as calculated [4] using Eq. (2), was 9 mΩ-mm².

$$R_s = \frac{1}{3} L^3 S^2 \frac{\rho}{wd} \quad (3)$$

where L is the finger length, S is the finger spacing, w is the width of the finger, d is the height of the finger, and ρ is the resistivity of the finger material.

The series resistance of our cells, without the wire bonds, was 10 mΩ-mm². As such, this points to a small contribution from the spreading and sheet resistance of the semiconductor.

The addition of a dielectric mirror between the semiconductor and the anode introduces challenges with respect to contact designs. Since the semiconductor is no longer in contact with a planar metal mirror at the back, grid patterns are needed at the back for carrier collection. This creates two challenges:

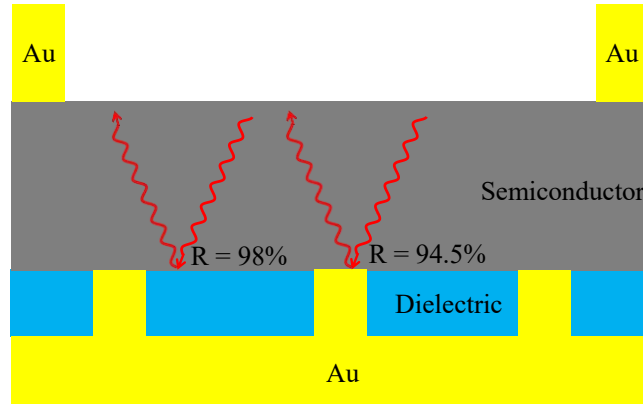


Figure 6. Device architecture with a dielectric spacer. Pinhole structures are needed in the dielectric layer to conduct the generated carriers from the semiconductor. Use of pinhole structure increases series resistance compared to a planar back contact.

(i) Reflectivity at the point of contact between gridlines and semiconductor will no longer be 98%, but 94.5%, as shown in Fig. 6. If we take a linear approximation for rear mirror reflectivity based on surface coverage of metals and dielectric, then the net reflectivity will be $R_{\text{eff}} = (1-f_c) R_{\text{sdm}} + f_c R_{\text{sm}}$, where R_{sdm} is the reflectivity of semiconductor-dielectric-metal (98%), and R_{sm} is the reflectivity of semiconductor-metal (94.5-95%). This net reflectivity combines both the specular and diffuse components. Electromagnetic simulation is needed to separate out the components from diffuse and specular reflectivity.

(ii) Series resistance also increases due to the structured contacts at the back.

Further optimization is necessary to obtain an optimum device geometry for higher reflectivity and lower series resistance.

2.3 Material Quality

Improved material quality leads to lower parasitic recombination inside the device. This leads to a higher open-circuit voltage, and as a result, higher thermophotovoltaic efficiency. Internal luminescence efficiency for our device was estimated to be 82%. The device material quality was mainly limited by Shockley-Read-Hall recombination. In the limit that defects are minimized such that Auger recombination takes over as the dominant parasitic recombination pathway, it is possible to obtain 98% internal luminescence efficiency.

2.4 Device and Chamber Geometry

Subtle effects arise from non-unity emissivity and view factor. Any photons that get reflected from the thermophotovoltaic cell will return to the emitter. For an emitter with non-unity absorptivity (corresponding to a non-unity emissivity, from Kirchhoff's law), this will cause cavity-like multiple reflections between the thermophotovoltaic cell and the emitter. Thus, a non-unity emissivity will effectively reduce the effective reflectivity for the sub-bandgap photons.

With an improved series resistance and mirror reflectivity, further gains in efficiency are possible through increased illumination on the photovoltaic cell. This increases the short-circuit current of the device. This can be achieved by the addition of an anti-reflection coating on top of the photovoltaic cell, as well as increasing the view factor from the emitter.

3 Conclusion

Highly efficient thermophotovoltaic power conversion is possible through spectral-filtering with the use of a rear-mirror. However, additional improvements, with regards to device design, are also needed to achieve power

efficiency~50%. Here, we have identified practical challenges to obtain 50% thermophotovoltaic efficiency and proposed some possible solutions along the way.

References

[1] Woolf, D. N. et. al., "High-efficiency thermophotovoltaic energy conversion enabled by a metamaterial selective emitter," *Optica*, 5(2), 213-218 (2018).

[2] Lenert, A. et. al., "A nanophotonic solar thermophotovoltaic device," *Nat. Nano*, 9, 126-130 (2014).

[3] Omair, Z. et. al., "Ultraefficient thermophotovoltaic power conversion by band-edge spectral filtering," *PNAS* 116(31), 15356-15361 (2019).

[4] "Finger Resistance," PV Education, 24 August 2019, < <https://www.pveducation.org/pvcdrom/design-of-silicon-cells/finger-resistance>>.